DESIGN CONSIDERATIONS FOR THRUST BEARING APPLICATIONS
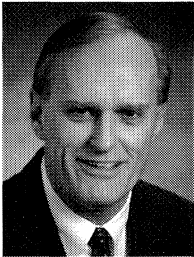
by

James H. Ball

Applications Engineer

Orion Corporation

Grafton, Wisconsin

James H. Ball received his B.S.M.E., M.S.M.E., and Ph.D. (Vibration Analysis and Mechanical Design) from University of Wisconsin-Madison (1965, 1971, 1975). While at the University of Wisconsin, he designed and analyzed a resonant vibratory machine for marine work. This included modelling viscous and coulomb damping.

Dr. Ball has been working in the bearing industry for 21 years. This includes five years as manager of product development at Waukesha Bearing Corporation and five years as an analyst at the Allis Chalmers Advanced Technology Center working on fluid film bearings. Rolling element bearing work occurred at Torrington Bearing Company and at the Bucyrus-Erie Company.

Currently, Dr. Ball is responsible for thrust bearing design and applications at the Orion Corporation, a company that manufactures tilting pad thrust and journal bearings, sleeve bearings, seal, and housed bearings systems for the rotating equipment industry for the last 40 years.

Dr. Ball, a member of ASME, STLE, and the Vibration Institute, has authored 12 technical papers concerning bearings, seals, pumps, tribology, machinery dynamics, and vibrations. He has five patents concerning fluid film bearings, seals, pumps, and vibration control.

ABSTRACT

The hydrodynamic thrust bearing load capacity-speed envelope is divided into three major regions by speed. Each region has its own set of limiting physical phenomenon that must be included in the analysis and presents a design challenge. For instance, the high speed region has high lubricant shear rates possibly including turbulence that change pad thermal crowning and local babbitt temperature and pressure, thus limiting the bearing performance in terms of load and speed. Various design tools are used to set the bearing geometry such that the phenomenon limits are not exceeded, and an appropriate design safety factor is present.

Several applications are presented that illustrate how the various design modifications such as pivot type, pivot radial and circumferential offset, pad spacing, and pad thickness may be varied to design a thrust bearing for a specific region. Three dimensional finite element models for the fluid film generate film thickness, pressure and temperature distributions, which when coupled with a pad finite element model for thermal conduction, convection, thermal deflection, and elastic deflection show thrust bearing pad performance. Turbulence is included along with hot oil carryover from the previous pad. Methods are shown that reduce vibratory motion by using the squeeze film damping attributes of double thrust bearings.

The benefits of offset pivot, chrome copper pads, and controlled lubrication in a load-speed region are reviewed so that the user has an appreciation of how each feature is affecting his thrust bearing's

performance. Of primary interest is an example of a high speed application where controlled lubrication increased machine efficiency by minimizing parasitic losses. Three dimensional maps of velocity, fluid mixing, temperature, and viscous heating in the pocket result in two dimensional temperature fields at the pad entrance. Accurate determination of the pad entrance temperature distribution allows for calculation of the pad maximum temperatures or bearing capacity. The examples and results presented will be of use to rotating equipment manufacturers and machinery users in applying thrust bearings to their machines.

INTRODUCTION

The thrust bearing babbitt maximum temperature is used to determine capacity for many designs. This is determined by the near fluid film temperature. The fluid film temperature increases by the action of the runner and pad shearing the oil. Thus film temperature is determined by adding an incremental temperature to the pad entrance temperature, which is a function of the energy generated in the fluid film between the pad entrance gap and the local maximum film temperature. Thus the film temperature at the pad entrance is a major factor in establishing bearing capacity. Historically the pad entrance temperatures have been a calculated single value.

Ettles [1] describes the pad entrance temperature in terms of a K factor in Equation (1).

$$T_1 = T_s + \Delta T \left(\frac{K_1}{2 - 2K_1} \right) \qquad (1)$$

Since the runner temperature is not known, it is usually taken as the mean of the pad streamline temperature. The limits for K are between .45 and .75 from field or laboratory tests on many thrust bearing types. Vohr [2] uses an energy balance to determine the pad entrance temperature. The shear energy generated is equal to the energy lost as side leakage, energy lost to the groove, pad, and runner. The bearing program iterates on the pad film properties until the entrance temperature satisfies.

$$E_T = E_G + E_R + E_P + E_S \qquad (2)$$

Heshmat and Pincus [3] describe a mixing function, λ, which is the deviation in percent between an ideal energy balance and experimented data. The function accounts for groove heat generation in and far from the runner boundary layer, heat fluxes at the walls, three dimensional effects such as radial and axial recirculation, and loss of some pad exit flow. Thus,

$$T_1 = \frac{Q_s T_s + Q_2 T_2}{Q_1 (1 + \lambda)} \qquad (3)$$

The mixing constant, λ, is fit to experimental data which results a function in terms of mean velocity and supply oil temperature. If recirculation is considered the equation becomes:

$$T_1 = \frac{(Q_s + Q_r)\, T_s + Q_2 T_2}{(Q_s + Q_r + Q_2)(1 + \lambda)} \qquad (4)$$

Recirculation was observed in bearings with inlet to outlet film ratios greater than 2.1. Thirty seven percent recirculation occurred when the ratio was seventeen to one. Dmochowski [4], et al., used a mixing equation to characterize conventional and pocket tilting pad journal bearings. The Heshmat and Pincus mixing function, λ, was set to zero so that the pad entrance temperature is:

$$T_1 = \frac{(Q_2 - Q_1)\, T_s + Q_2 T_2}{Q_1} \qquad (5)$$

for conventional bearings. For the pocket bearings the pad entrance temperature is:

$$T_1 = \frac{Q_s T_s + (Q_1 - Q_s) T_2}{Q_1} \qquad (6)$$

The difference being that for the pocket bearing, it is assumed that all the supply flow, Q_s, is taken by the pad entrance gap; whereas, in the conventional bearing all of the pad exit flow, Q_2, is taken by the pad entrance gap to 90 percent of the entrance flow, Q_1. Dmochowski explains pad entrance temperature equations for the two bearings in terms of a stratified temperature of fluid at the pad entrance gap. His hypothesis for Equation (1) and Equation (2) was based on noting that experimentally the outlet temperature for the conventional bearing did not change with variation in flow as it did for the pocket bearing.

With the increasing use of computational fluid dynamics (CFD) the pad entrance temperature could be considered a two dimensional array that would include consideration of the hotter boundary layer oil near the runner and between pad mixing. Pad entrance backflow and recirculation effects that occur because of the stationery pad and the wedge shape of the film could be included. The thermal and elastic pad deflection at the front edge would cause the gap to vary with radius; the array could include this effect. Prepad features such as wipers and directors could be modelled from a fluids view and their effects on pad entrance temperature considered. The CFD tool appears to refine the determination of the pad entrance temperatures by modelling fluids phenomenon in greater detail. This approach is used for pad entrance temperature calculations in a controlled inlet tilt pad thrust bearing design.

A controlled inlet thrust bearing that features a cool oil cavity for the pad entrance oil along with a hot oil carryover director and wiper is discussed. The oil feed system includes a hydraulically actuated piston between the pad and retainer to transfer the oil to the cool oil cavity. The thrust bearing is thin because of the retainer and equalizing link design. The design features augmented bearing capacity and efficiency.

Design and analysis of equalized tilting pad thrust bearings is reviewed so that rotating equipment users can operate machines at higher reliability. Rotating equipment manufactures with an increased awareness of current tilt pad thrust bearing performance parameters and design features could lower machine bearing costs or increase machine safety factors. Users with an increased understanding of how tilt pad thrust bearing performance parameters were obtained can review bearing reserve capacity or decide on whether or not a higher capacity bearing is needed for a rerate. If a capacity increase is needed that could occur in the same envelope by adding bearing features to the same bearing envelope, that would save housing and shaft modifications.

The bearing load speed map should be used as a guide to determine which tilt pad bearing performance parameters are

limiting capacity. The various regions require alternate design solutions to optimize bearing capacity. For some applications, especially process fluid bearings, a film thickness to surface parameter ratio is a better parameter than film thickness to set capacity limits. When tilt pad thrust bearings run unloaded, system vibration can occur. Users can make several adjustments to reduce the vibration. When bearing designers size a bearing, the analyses are varied and, in some cases, answers can differ by more than 100 percent. Both users and machinery builders should be aware of the differences so that a base level comparison can be made for capacity at speed with a bearing manufacturer's different features or different bearing manufacturers.

Various bearing features can effect load capacity. Knowledge of the features and their relationship with capacity would also help in bearing selection. The pad ratio, pad spacing, pad crowning both elasticity and thermally, pad height, button diameter, and button thickness effect capacity. The babbitt pressure and temperature is related to bearing failure by creep. By making slight changes to the pivot position bearing temperature and film thickness deficiencies can be corrected.

CONSIDERATIONS IN TILT PAD BEARING SELECTION PROCEDURES
Applications

There are numerous considerations to resolve when reviewing a thrust bearing application (Table 1). The ratio of minimum film thickness to surface finish should be reviewed for process fluid bearings. The degree of misalignment present especially for non-equalized bearings can load less than the full complement of pads. Pad height will effect crowning, which influences load capacity. On large pads, can button recess diameter improve crowning? What is the safety factor with babbitt creep? What design features can be used to augment capacity in the same envelope? How do offset pads, copper pads, and controlled inlet lubrication affect thrust capacity. How can the maximum pad temperature be reduced by changing the oil feed supply? What are the parasite power losses for a flooded design? Would a thin section bearing be applicable here? What is the safety factor for stress at the pad pivot and link pivots? What is the shock capability of the bearing, time duration, film thickness, and babbitt pressure? For a double thrust bearing, how does the damping reduce unloaded vibration? What is the film and mechanical stiffness of the bearing and how do they add to give an equivalent bearing stiffness? What thermal crown exists on the pad in each of the three regions of the load speed map? The pivot radial location is important to minimize film temperature or maximize film thickness. The circumferential location changes film temperature, film thickness, and film pressure. The pad length (parallel to rotation) to width ratio can change film temperature by shortening the streamline length under shear in the film. Changing the pad entrance temperature affects the minimum film thickness. Various pad support designs can reduce pad elastic deflection. Is film turbulence occurring? At what level is it, especially for additional power loss estimates? If the bearing is running starved, how did film pressures increase towards the trailing edge of the pad?

The thrust bearing will operate in one of three liquid lubrication regions. The region location is shown in Figure 1 for boundary, mixed, and hydrodynamic modes. Boundary lubrication is defined by metal to metal contact and wear. The PV value, or unit pressure times velocity value, with pressure and velocity limits establish wear limits for this region. A material pair that runs hard on hard, such as CVD diamond coated pads and runners, would be suitable here. Hydrostatic lubrication is an alternative to wear designs at these speeds.

Hydrodynamic lubrication is complete separation of the runner and bearing pad by a film of oil. Mixed lubrication is aptly titled

Table 1. Application Variables Affecting the Load/Speed Map.

NO.	VARIABLES	REGION 1 FILM THICKNESS	REGION 2 UNIT PRESSURE (LOAD)	REGION 3 TEMPERATURE
	APPLICATION:			
1	ROUGHNESS, SURFACE FINISH	1		
2	FLATNESS/WAVINESS, SURFACE FINISH	1		
3	RUN IN	1		
4	MATERIAL PAIR	1		
5	LUBRICANT VISCOSITY	1		2
6	ALIGNMENT	2	1	
7	STARVED OIL SUPPLY		1	
	DESIGN:			
8	OIL SUPPLY, QUANTITY		2	1
9	OIL SUPPLY, TYPE			1
10	TURBULENCE			1
11	NUMBER OF PADS/PAD SPACING	2		1
12	PAD RATIO		2	1
13	PIVOT FATIGUE		1	
14	ELASTIC CROWNING	1	2	
15	THERMAL CROWNING			1
16	CREEP LIMIT		1	2
17	COPPER PADS		2	1
18	OFFSET PIVOT			1

INTENSITY AFFECT UPON DESIGN
1 = HI   2 = MEDIUM   3 = LOW
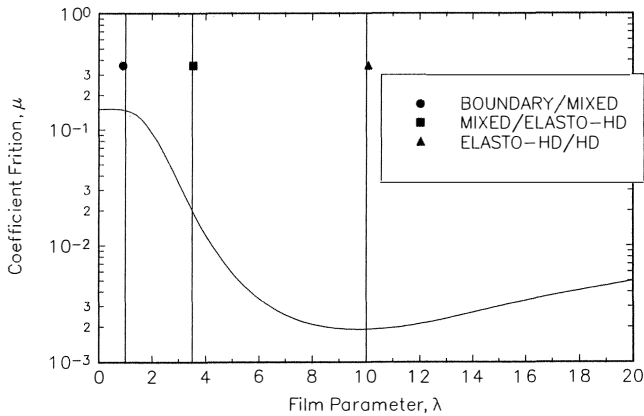
Figure 1. Lubrication Regime Map.

and occurs between the two regions. Notice that the map is a plot of friction coefficient vs the film ratio, which is a ratio of liquid film to pad and runner surface finish. The map is the same if the abscissa is a duty parameter, μ N/P, or the Sommerfeld number.

When thrust bearings are applied in the hydrodynamic region, as speed increases the bearings are limited by different phenomenon (Figure 2). At low speeds adjacent to the mixed film region, film thickness limits the load. A central region exists where the bearing is load limited by the bearing features. At high speeds, capacity is film and bearing material thermal limited. For petroleum lubricants, the oxidation limit is about 300°F and babbitt has a limit of 265°F.

The film exhibits primarily viscous forces in the low speed region. For different wedge shapes, Reynolds equation can be solved for the pressure distribution the film generates to support
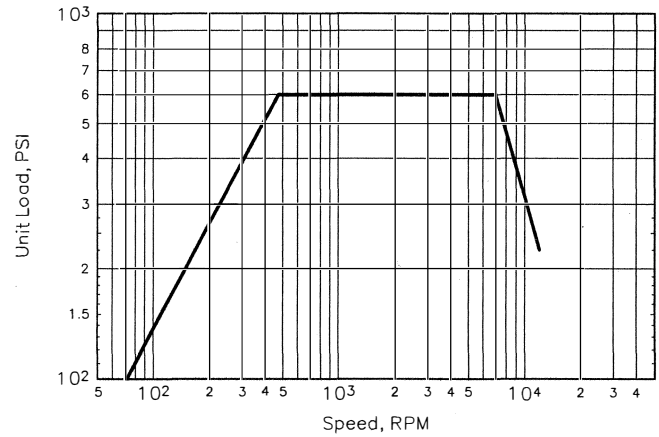

Figure 2. Thrust Bearing Load Vs Speed Capacity Map.

the load. For the intermediate region that is load limited, the energy and Reynolds equation need to be used in the solution, since temperature effects viscosity greatly. The energy equation yields film temperature so that the local viscosity can be used in the Reynolds equation for the load solution. When speeds are higher, turbulence needs to be accounted for in the analysis. This is accomplished by adding Hirs constants to the Reynolds equation.

The low speed region that is governed by the minimum film thickness has a positive slope. Thus, load is reduced or limited. The nominal limit is 250 micro in. The limit is based on surface finish produced by the different manufacturing process. Assume that the pad will mirror the surface finish of the runner after run in and that the film thickness should be greater than the irregularities in both surfaces. Process surfaces are characterized by root mean square or average profilometer roughness, predominant peak roughness, and peak to trough maximum roughness. Tarasov, as noted by Ocvirk [5], found that processes had different ratios of predominate peaks roughness/RMS roughness ratios. Martin [6], used this value with a safety factor of two for minimum film thickness design criteria. For example, if the runner was ground, the minimum film thickness would be: 16 RMS $\times$ 4.5 $\times$ 2.0 $\times$ 2.0 = 288 micro in. The value varies with pad width or bearing size when based on predominant peek ratios where at a pad width of 0.5 in for a 4.0 in bearing, the limit value is 180 micro in. This increases to a recommended minimum film thickness of 550 micro in for a 25 in bearing with a 6.25 in pad width. Using a higher viscosity lubricant in this region can raise the film to an acceptable value, since the film is not running at high temperatures. Changing from a full pad complement to a partial pad complement can reduce the pad entrance temperature, thus raising film thickness. For instance, a complement of six vs twelve pads reduces the pad inlet temperature 17 percent.

The intermediate speed region is limited by bearing unit pressure or load. The load affects the limits of the components. For instance, as load increases, elastic crowning increases, which decreases bearing capacity. As load increases, pivot radii need to be increased or pivot fretting will occur. As load increases, the babbitt creep limit is approached due to the material local pressure-temperature relationship. Misalignment can cause fewer pads to share the load in nonequalized bearings, which can overload the working pads. A starved bearing causes a percentage of the pad to support the load rather than the whole pad, thus changing the babbitt pressure temperature profile with regard to the creep limit.

The high speed region loads need to be reduced due to local babbitt temperature where wiping starts at about 265°F. Thermal crowning is dominant when compared with elastic crowning in this region which reduces capacity. Increasing the pad spacing can

lower babbitt temperatures by dropping pad entrance temperature, which occurs because the hot oil carryover boundary layer oil has more time to mix with the feed oil. Turbulence is occurring in this region that can retard babbitt temperatures for several thousand rpm before continuing to rise as a function of speed. Power dissipation also increases with speed. At a Reynolds number of 550, turbulent power loss equals the laminar shear loss; at 1100, the turbulence loss is double the shear loss.

High speed machinery with double thrust bearings running in an unloaded condition can have axial vibration due to a forced response. The vibration occurs at the shaft/bearing natural frequency and can have a double amplitude less than, or equal to, the bearing float or clearance. By reducing the clearance, the thrust bearing pads add damping to the single degree of freedom shaft/bearing vibratory model. Some reduction in the clearance adds sufficient damping, usually to reduce the vibration to acceptable levels. A graph is presented in Figure 3 of thrust bearing damping ratio *vs* clearance used to adjust the axial float to reduce vibration.
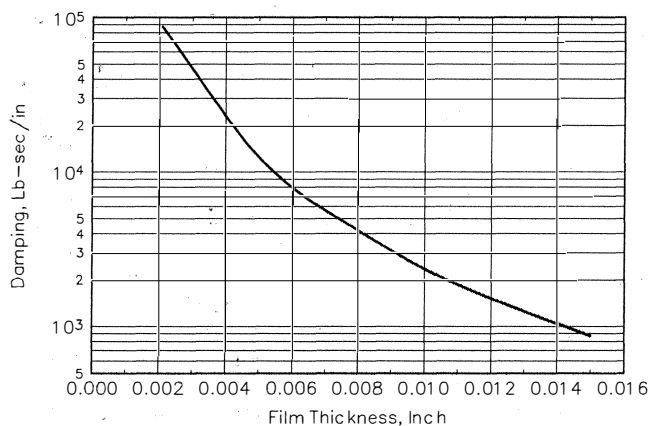
Figure 3. Thrust Bearing Axial Damping.

Bearing Analysis Procedures

There is an abundance of analysis procedures for tilt pad thrust bearings. Historically closed form equations with a constant viscosity were used as with the one dimensional infinite slider equations for load capacity, friction, and center of pressure. With computers came the ability to include two or three dimensional modelling, modelling additional phenomena with interactions, and reasonable time frames to solve a specific application. All analyses solve the film Reynolds equation (A-1) for the pad pressure distribution given the wedge geometry. The wedge geometry for the pad is represented by a circumferential and radial tilt. This tilt is iterated until a pad pressure distribution is found that will support the load. Since the viscosity temperature gradient is high and nonlinear, a more accurate solution to the hydrodynamic problem involves solving the energy equation with the Reynolds equation. This increases the computational requirement that is easily handled with today's personal computers and engineering work stations.

Now other phenomena can be modelled to give results that correlate with experimental data. Pad elastic deflections due to the load and thermal differential through the pad are important in terms of crowning effects on load capacity. This can also be the case for the runner. Turbulence can be approximated with the Hirs coefficient which is incorporated into the Reynolds equation.

The various analyses are summarized below:

• Isoviscous approximation by closed form solutions for film, i.e., short or long bearing theory

• Isoviscous hydrodynamic film solution

• Thermohydrodynamic film solution

• Thermohydrodynamic film solution with turbulence

• Thermohydrodynamic film solution with turbulence and pad thermal effects

• Thermohydrodynamic film solution with turbulence and pad elastic effects

• Thermohydrodynamic film solution with pad thermal and elastic effects

• Thermohydrodynamic film solution with pad and runner thermal and elastic effects

• CFD coupled thermohydrodynamic film solutions with pad and runner thermal and elastic effects

The various analyses can be one, two, or three dimensional. In today's bearing market, most of the effects should be included in the analyses that is part of the tilt pad thrust bearing application work.

A comparison was made of bearing film thickness for various analyses types shown in Table 2 for a 10-1/2 in eight pad bearing running at 10,000 rpm and loaded to 635 psi (35,000 pounds). The program used to generate the performance parameters uses finite element methods to solve a two dimensional Reynolds equation with turbulence and groove mixing. The energy equation is solved in three dimensions and is also finite element which allows for cross film viscosity variation. The pad uses a three dimensional thermal conduction/convection finite element model and an elastic finite element model. Heat flux from the film to the pad uses temperature gradients from the energy equation solution. Varying geometry can occur in the pad. The runner model is axisymmetric for both the thermal and elastic case. Turbulence is included in Reynolds equation by Reichardt's Formula for the eddy viscosity. The energy equation has modified local conductivity and viscosity for turbulence.

Notice that the energy equation is used to find maximum film or babbitt temperature which is an indication of bearing capacity. Crowning can effect capacity; therefore, pad deflection both thermal and elastic should be added. This reduces the minimum film thickness by 35 percent when compared to the isoviscous case, Table 2, Case 1 *vs* 6. All these effects should probably be included in a tilt pad thrust bearing application review. By allowing the viscosity to vary with temperature, the minimum film thickness decreases by 47 percent and the horsepower by 25 percent for a rigid pad when compared to the isoviscous case, Table 2, Case 1 *vs* 3. The film thickness increases 23 percent from the Reynolds/Energy solution when pad effects are added, Table 2, Case 3 *vs* 6. The elastic pad causes film thickness to increase. Brockett [7] found little change in the film thickness when considering runner mechanical deformation for a typical runner thickness. The addition of turbulence effects increased the maximum temperature and horsepower loss values. Thus, when comparing bearing manufacturer's data, the question of analysis type should be asked.

Typical pad plots are shown in Figures 4, 5, 6, 7, and 8. The plane view is shown in Figure 4 of the film pressure distribution. The film thickness with isoclines is shown in Figure 5. The three dimensional film temperature distribution is shown in Figure 6. The pad temperature distribution and elastic deformation are shown in Figures 7 and 8.

Design

Pad design determines the tilting pad bearing capacity. The pad crowning ratio and babbitt strength are criteria that are considered along with minimum film thickness. The maximum bearing

Table 2. Thrust Bearing Performance by Analysis Type.

	REYNOLDS EQUATION	ENERGY EQUATION	TURBULANCE	PAD THERMAL EFFECT	PAD ELASTIC EFFECT	RUNNER THERMAL EFFECT	RUNNER ELASTIC EFFECT
1	1D 2D						
2	2D	3D					
3	2D	3D	X				
4	2D	3D	X	X			
5	2D	3D	X		X		
6	2D	3D	X	X	X		
7	2D	3D	X	X	X	X	
8	2D	3D	X	X	X		X
9	2D	3D	X	X	X	X	X

Figure 5. Typical Pad Film Thickness Distribution.
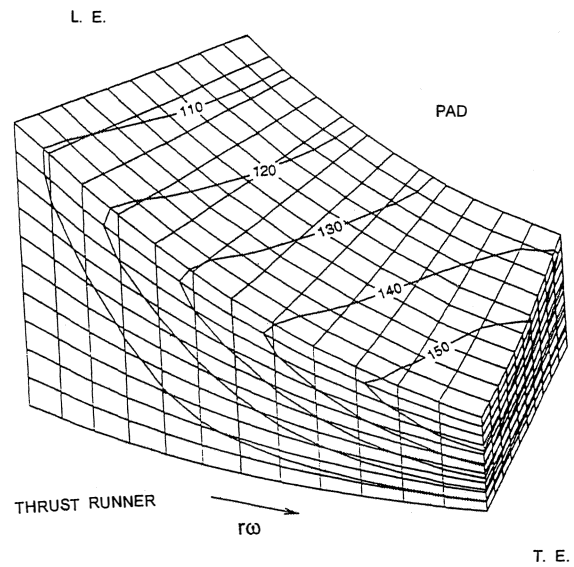
Figure 6. Typical Pad Film Temperature Distribution.

Figure 4. Typical Pad Film Pressure Distribution.
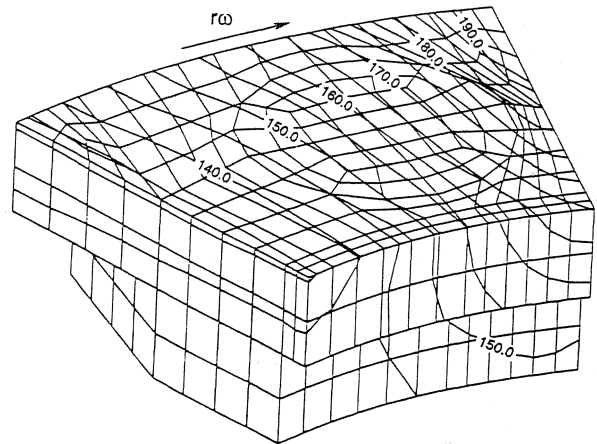
Figure 7. Pad Temperature Distribution.
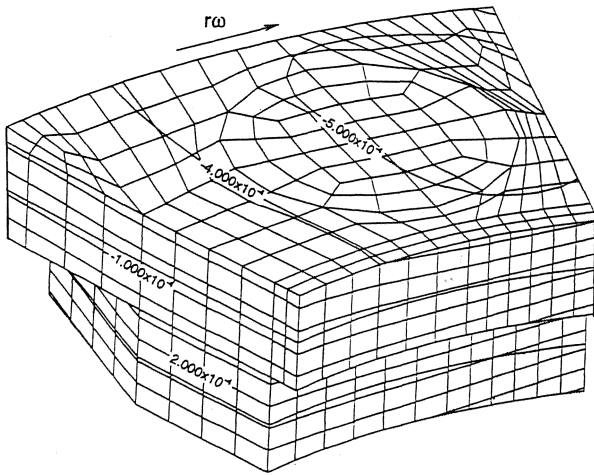
Figure 8. Pad Elastic Deformation.

capacity is related to the pad crowning ratio and at this load the babbitt has a pressure/temperature creep limit that is considered. The pad thickness and pivot type and geometry influence crowning. Pad spacing affects pad entrance temperature, thus maximum capacity. The maximum temperature and minimum film thickness positions on the pad are affected by the circumferential and radial pivot position. The pad ratio which is pad width, length transverse to the flow, over mean circumferential length, shear streamline length, which is tangent to the flow direction, affects maximum babbitt temperature. Horsepower loss reflected in the bulk temperature rise and required oil supply and temperature are system variables that the machinery builder and user require to specify the bearing lubrication system.

Thrust bearing capacity depends on pad distortion and minimum film thickness. Distortion is the maximum height of the pad surface curvature from a line connecting the opposite pad edges. Raimondi found that the load variable was maximum at a crown to minimum film thickness ratio of 0.6. For center pivot thrust pads that depend on elastic curvature to support the load at start up, crown ratios below 0.5 show a steep reduction in load capacity. For crown ratios above 0.6 the reduction in capacity occurs but at a slower rate. The load capacity is shown in Figure 9 as a function of crowning ratio.
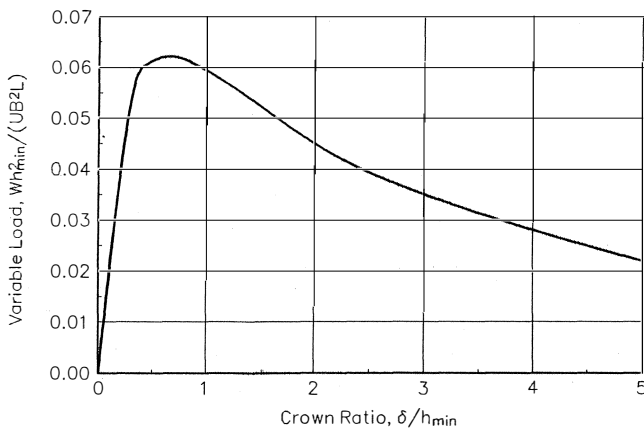

Figure 9. Load Variable Vs Crown Ratio for a Center Pivot Thrust Bearing.

Babbitt creep occurs at elevated local temperatures and local pressures through the hydrodynamic film. Booser [8] correlated wiping or creep with babbitt yield that is temperature dependent

(Figure 10). The low film tangential shear forces create babbitt flow due to sub surface shear at high yield stresses. A bearing load line can be superimposed on this graph to determine at what load and speed the babbitt will creep and a safety factor can then be applied. This assumes that the same pad surface node is always the node of maximum temperature and pressure. This is not the case, in fact the maximum pressure and temperature are occurring at different nodes. Also, as the pad load or speed increases, the thermal and elastic deflections cause the positions to change. Thus, each node with its respective temperature and pressure should be compared to the pressure/temperature creep limit for each load and speed condition.
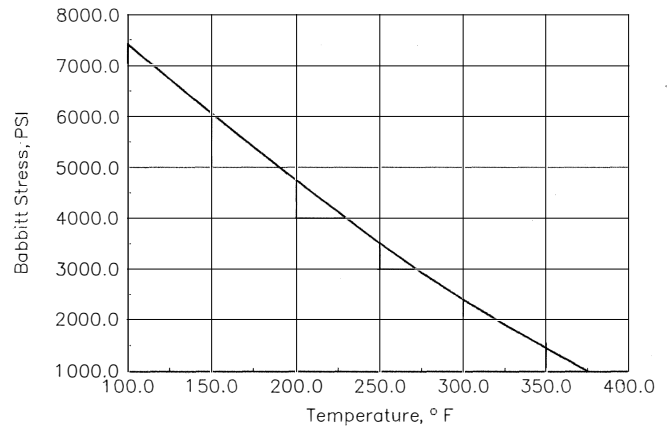

Figure 10. Grade 2 Babbitt Yield Vs Limiting Temperature.

Pad thickness affects load capacity. At maximum capacity the ratio of crown to minimum film thickness is 0.6. Assuming a film thickness of 0.001 in, the pad elastic crown should be 0.0006 in. With the criteria and deflection equations, the pad height may be determined. This results in pad heights approximately one-fourth of the equivalent pad diameter.

The pad ratio affects the bearing parameters. The pad ratio, which is the mean circumferential pad length over pad radial width, influences the temperature rise across the pad. Using a one dimensional energy equation and Reynolds equation in the direction of motion for an adiabatic film will give the temperature rise of a laminar film. For turbulent films, the temperature rise is computed with a turbulent fluid friction factor and an equivalent viscosity that is a function of Reynolds number. When comparing a six and eight pad 10-1/2 in thrust bearings, the maximum babbitt temperature of the six pad with a mean streamline of 3.5 in is approximately seven percent higher than the eight pad with a 2.63 in mean streamline. The pad ratio affects the load capacity and film thickness because of side leakage. The pad horsepower loss is different since the friction factor changes with pad ratio.

Pad spacing can affect the inlet temperature; thus ultimately influencing pad maximum temperature or capacity. The relation is shown in Table 3 of different bearing variables to Ettles' hot oil carryover coefficient. The table was a result of 597 tests with tilt pad thrust bearings. By decreasing the number of pads in a thrust ring in increments of two, from 12 pads to four pads, the carryover coefficient, K_1, was reduced from 0.77 to 0.51. Using Equation (1), the pad inlet temperature drops by 46°F for the four pad bearing compared to the 12 pad. In changing from an eight to six pad, the pad entrance temperature drops 12°F. Note that the design change of the number of pads is as significant as load change for the range tabulated.

Various pivot designs can be used to support the pad: point contact, ring contact, and line contact. Point contact as a sphere on

Table 3. Tilt Pad Hot Oil Carryover Vs Thrust Bearing Parameters.

APPLICATION/DESIGN PARAMETER	K	ΔK
OVERALL	.67	
4000 REV/MIN	.60	
6000 REV/MIN	.68	.13
8000 REV/MIN	.73	
NUMBER OF PADS		
4	.51	
6	.63	
8	.70	.26
10	.72	
12	.77	
FLOW, GAL/MIN		
2.74	.70	
5.42	.66	.04
8.25	.66	
OIL TEMPERATURE RISE ACROSS HOUSING, °F		
10-20	.51	
20-30	.59	
30-40	.62	
40-50	.70	.28
50-60	.74	
60-70	.79	
70-80	.78	
SPECIFIC LOAD, LBF/IN²		
0-200	.69	
200-400	.73	
400-600	.66	.28
600-800	.61	
800-1000	.60	
1000-1200	.45	

plate can be used in low to medium loaded thrust pads. Large pads, especially that start under load, use a ring contact. Raimondi found that a support ring radius to pad equivalent radius of one-third was appropriate when considering elastic deflections. This design has an intermediate disc with ring contact at the pad and point contact loading the link. Ratios greater than 0.56 cause poor lift because the pad surface is concave. Ratios near zero cause excessive pad edge deflection. A ratio of one-third is optimum for considering both pad edge deflection and concavity. At operating conditions, the addition of thermal deflections result in a completely convex surface.

Pads with radial line contact extending the width of the pad increase bearing capacity. The line contact reduces pad edge deflection compared to the point and ring contact. This causes capacity to increase. For a center pivot bearing with a pad ratio of one, Raimondi, Boyd, and Kaufman found the maximum capacity at the optimum crown to minimum film thickness ratio to be 30 percent greater for the same film thickness.

The pad pivot can be located by different criteria. The circumferential offset of the pivot from the pad entrance is a ratio with the mean circumferential length of the pad. As the offset is increased from 0.50 for center pivot, the maximum temperature drops and the film thickness increases. The minimum peak babbitt temperature occurs at pivot offsets between 75 percent and 85 percent when determined experimentally. The range accounts for different designs. At this offset, the local film pressures are greater and the minimum film thickness is somewhat lower.

The radial offset tilts the pad to the outside or inside depending on its location. The pivot radial offset ratio is defined as the radial distance from the babbitt bore to the pivot location divided by the pad width. The center of pressure of the film is at a greater radius than the pad geometrical center. An outward tilting pad does have benefits even though a fixed compound taper land thrust bearing has an inward tilting pad. Varying the radial tilt angle by moving the pivot, the maximum local film temperature position can be moved and reduced. Also the film thickness can be increased by moving the pivot radially. By changing the pivot radius, the temperatures and film thickness of the pad trailing edge may be optimized such that the pad trailing edge values are approximately equal between the pivot and the babbitt outside diameter.

PAD ENTRANCE TEMPERATURE DETERMINATION WITH CFD ANALYSIS

CFD Analysis and Procedures

A computational fluid dynamics analysis of the inlet and near geometry was completed to compare the pocket performance under laminar and turbulent flow conditions. Tucker and Keogh [9] use CFD methods to study shaft thermal bowing in journal bearings while forward and backward whirling was occurring. San Andres, et al. [10], used CFD methods to investigate thermal behavior of cryogenic seals.

Computational fluid dynamics solves the fluid continuity Equation (A-2) or (A-6), the momentum equation (A-3) or (A-7), and the energy equation (A-5) or (A-8). Since flow in the cavity is turbulent, the analysis uses (A-7) and (A-8). The difference between the laminar and turbulent momentum equations is the viscosity. The laminar analysis viscosity is a function of temperature while the turbulent analysis uses an effective viscosity that is the sum of laminar and turbulent viscosities. The energy equation differs in that turbulent kinetic energy is included in the total enthalpy for the turbulent case. The conduction term of the turbulent energy equation includes the partial derivative of the enthalpy and a shear heating term is added that includes terms from the turbulent k-ε model.

The mixing of the fluid in the cavity was modelled as mass fractions of the fluid entering at inlet one and two. The solution of the momentum transport Equation (A-9) with the mass fraction scalar shows mixing as a tracer dye from inlet two. The Spaulding and Launder model (k-ε) was used for determination of kinetic energy and kinetic energy dissipation rate in the turbulent fluid. Both the kinetic energy and the dissipation rate of the energy are solved as scalar quantities in the momentum transport Equation (A-10) and (A-11). This allows us to predicate the fluid shear heating. The major component of heating is the viscous heating represented by Equation (A-12).

The fluids finite element solution is three dimensional and a fully coupled solution of the Navier-Stokes and energy equation at each node. Each fluids model has approximately 100,000 nodes which form six sided hexahedral (brick) elements. Solution includes centrifugal effects and swirl effects of the runner on the fluid and viscous shearing effects in the fluid. At each node, the velocity in three mutually perpendicular directions, k-ε turbulence, pressure, and temperature were calculated. The laminar viscosity of the fluid was modelled as a function of temperature. The boundary layer near walls is viewed as a near wall laminar flow (Law of the Wall) and a sublayer turbulent flow (Log Law of Wall). Selected plots are from a group of plots that show temperature, mixing, and velocity in the two orthogonal directions longitudinally and three planes in the transverse direction.

Pad Entrance Temperature Problem

In the two cases reviewed, a comparison of a control inlet pocket bearing at high speed but laminar, Case A, was made with the same controlled inlet bearing running under turbulent conditions, Case B. The film Reynolds number is 610 for the laminar and 1510 for the turbulent case. The 10-1/2 in, eight pad bearing is lubricated by

ISO VG-32 oil. The OD/ID ratio is two and the pad length to width ratio is one. The bearing has copper pads with a 68 percent pivot offset. Static performance data for the two cases are shown in Table 4

Table 4. Comparison of a Control Inlet 10-1/2 in 8 Pad Thrust Bearing Under Laminar and Turbulent Conditions.

CASE	DESCRIPTION	SPEED RPM (FPS)	LOAD LB	PRESSURE PSI	MINFILM INCH	POWER LOSS HP	OIL REQD GPM	BULK TEMP RISE °F
A	CONTROL INLET LAMINAR	10000 (343)	35000	635	.00079	75	19	50
B	CONTROL INLET TURBULENT	17000 (583)	35000	635	.0013	223	56	50

The controlled inlet bearing pocket CFD analysis between pad geometry is: a precavity to direct hot oil carryover radially out of the bearing, a hot oil director wall to shed some boundary oil, a land to wipe some of the boundary oil off the runner and, of course, the cool oil pocket to add cool oil such that the mixed temperature of the pad inlet is lower than a flooded bearing. The advantage of the controlled inlet in general is that inlet oil at 120°F, rather than a bulk temperature oil equal to the outlet oil at 150°F, is mixing with the boundary oil. The offset pivot drops the pad front edge or inclines the pad more so that the ratio of pocket oil to boundary oil is higher, allowing for a lower resultant or mixed pad inlet temperature.
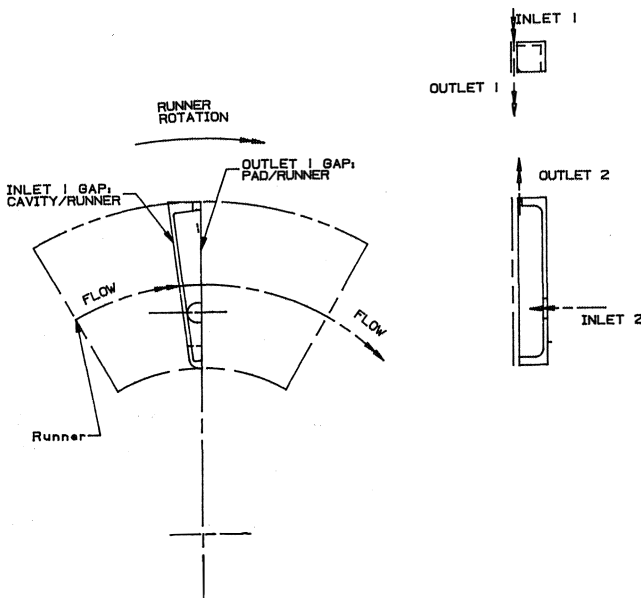
Figure 11. CFD Cavity Model Including Inlet/Outlet Locations.

The controlled inlet has four boundaries, Figure 11 and Figure 12, where the flow (velocity field), temperature, and pressure are specified. Inlet one sees hot boundary oil from the previous pad and recirculation. The temperature and gap between the pocket front edge and runner vary with radius. The temperature can be partially determined from the pad thermoelastohydrodynamic analysis. The pad outlet temperature and velocity boundary layers are used. The boundary layer temperatures are used with back flow temperatures set to the pre-cavity average temperatures. The thermal and elastic deflection along with pad tilt set the gap. Back flow is also occurring. Couette flow and runner speed determines
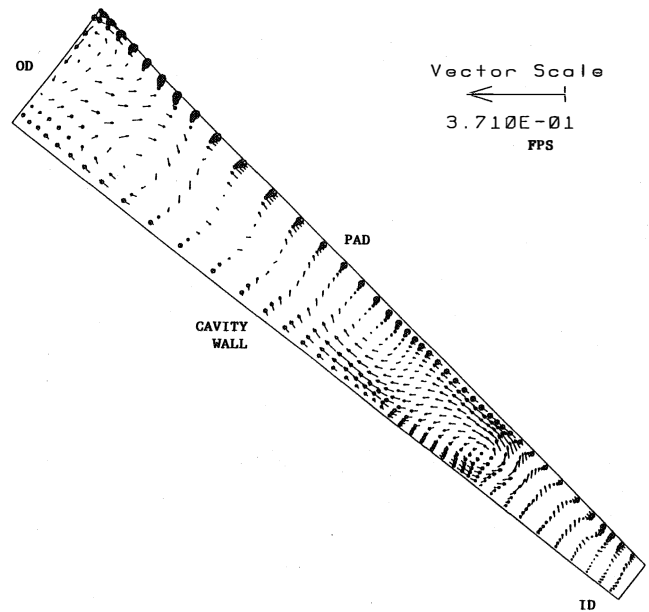
Figure 12. Controlled Inlet Pad Cavity Axial Mid Plane Laminar Velocity Field (.188 in from Runner).

the velocity distribution where back flow velocity is set to zero. Inlet two is for the fresh oil. This is at a temperature of 120°F and the flow is the required for hydrodynamic lubrication. The pressure is assumed to be zero psig, which is the most conservative assumption producing the highest pad inlet temperatures. Higher pressures will drop the inlet temperature.

At outlet one, the gap is determined by pad tilt and thermal and elastic deflections. The pressure is obtained from the pad hydrodynamic analysis. Recirculation of the flow occurs. The CFD analysis determines the gap field temperatures, proportion of recirculation, and flow velocity distribution to the pad. Outlet two is for excess flow bleed off.

Pad Entrance Temperature Solution

The CFD model for laminar Case A had the following fluid properties: swirl at the mid plane in a plane parallel to the runner was occurring at inlet two (Figure 12). Three vortices were occurring near outlet two. Average flow velocities were approximately 11 percent of runner velocity with a maximum velocity of 26 percent of runner velocity. The radial mid plane, perpendicular to the runner, velocity field was toward the runner at inlet two and two vortices were present at outlet two (Figure 13). The vortex near the outlet was feeding the outlet while the adjacent vortex was of opposite rotation and lower in the pocket. The average field velocity was near seven percent of runner velocity. The transverse velocity field at the optimized pocket section was centered at the pocket center and swirl was adding cool oil to the moving boundary layer feeding the pad (Figure 14). The core rotation factor is 4.2 percent of the runner velocity.

Temperatures for the pocket in the three planes were greater than the inlet two temperatures (Figures 15, 16, and 17). Entrance zone temperatures were near the 120°F inlet two fluid. They extended for the middle one-half of the pocket in axial and radial mid planes. The outer transverse section was warmer than the mean and inner transverse sections:

Tracer dye injected at inlet two is fully mixed at smaller radii (Figure 18). At larger radii, mixing increases from 75/25, 65/35, to 50/50 in the axial plane. This is also the case on the radial plane (Figure 19). At the optimum transverse plan mixing to the 50/50 is occurring near the boundary layer (Figure 20).
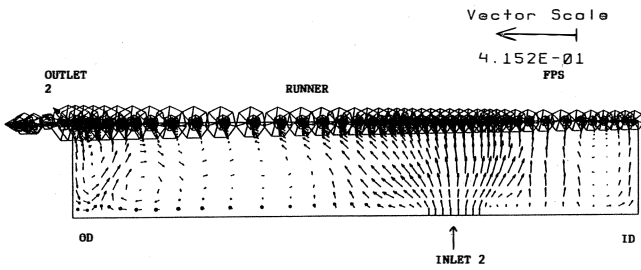
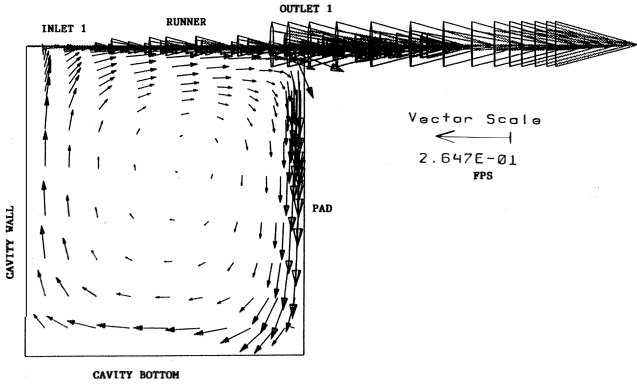Figure 13. Controlled Inlet Pad Cavity Radial Mid Plane Laminar Velocity Field.

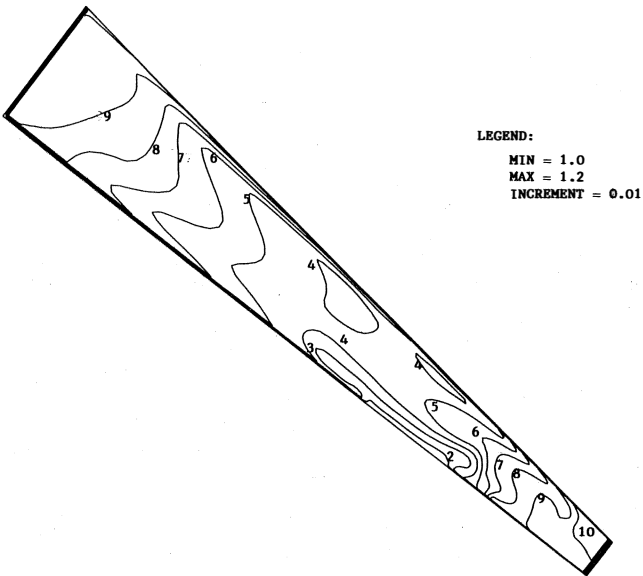Figure 14. Controlled Inlet Pad Cavity Transverse Plane Laminar Velocity Field (Radius = 4.54 in).

Figure 15. Controlled Inlet Pad Cavity Axial Mid Plane Temperature Distribution for Laminar Flow.

Figure 16. Controlled Inlet Pad Cavity Radial Mid Plane Temperature Distribution for Laminar Flow.
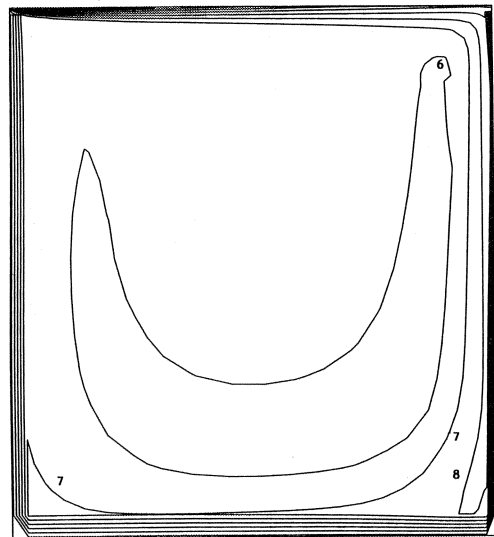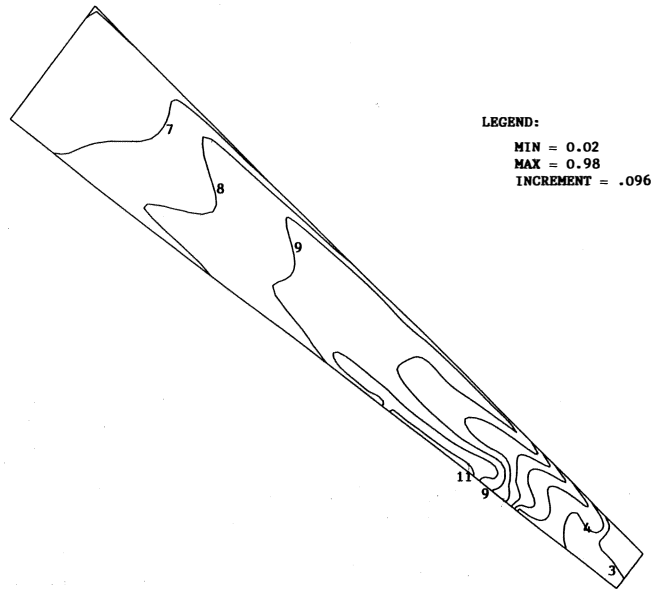
Figure 17. Controlled Inlet Pad Cavity Transverse Plane Temperature Distribution for Laminar Flow.

Figure 18. Controlled Inlet Pad Cavity Axial Mid Plane Mixing Field for Laminar Flow.
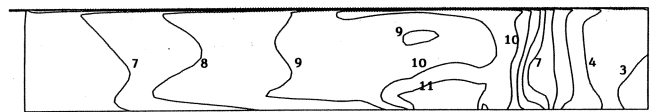
Figure 19. Controlled Inlet Pad Cavity Radial Mid Plane Mixing Field for Laminar Flow.

Viscous heating is occurring in the boundary layer or near it and at the pocket pad wall in a zone that is not large (Figure 21). The horsepower generated by the pocket is 0.016 per pad, which raises the oil temperature 0.1°F.
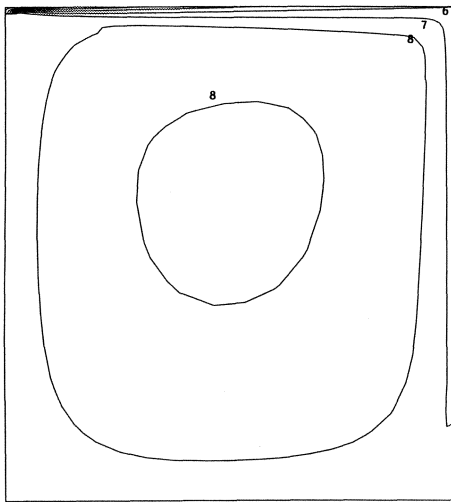
Figure 20. Controlled Inlet Pad Cavity Transverse Plane Mixing Field for Laminar Flow.
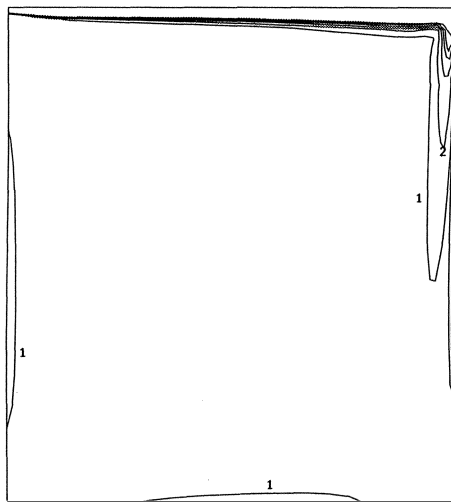
Figure 21. Controlled Inlet Pad Cavity Transverse Plane Viscous Heating for Laminar Flow.

The pocket/pad feed interface plane, outlet one, dominant velocity is at approximately 40 percent of runner velocity (Figure 22). The hot boundary layer has been reduced to five percent of the gap at the pad bore and 10 percent of the gap at the pad O.D. Back flow averaging 15 percent of runner velocity occurs to 50 percent of the gap at the pad bore due to low tangential velocity and 50 percent of the gap near the pad O.D. due to outlet two. Back flow is less than 12 percent for 65 percent pad width centrally located.

LEGEND:
MIN =−0.52
MAX =+1.31
INCREMENT = 0.37
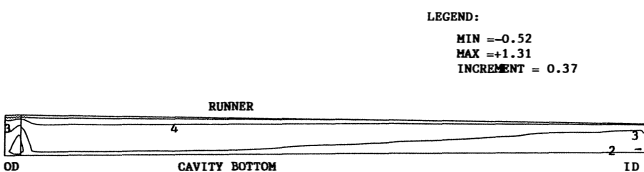
Figure 22. Pad with Pocket Inlet Velocity Field for Laminar Flow (Pad Entrance Gap, Outlet 1).

The pocket/pad feed plane temperature distribution shows a central area of cool oil 35 percent of pad width and 80 percent of the gap at 1.07 times the bearing supply oil (Figure 23). Zones on both sides are at 1.17 times supply oil, the inner zone is 10 percent wide and 80 percent of the gap while the outer zone is 40 percent wide and 80 percent high. The boundary layer temperature is 1.2 times supplied temperature, the length of the pad for 12 percent of the gap. The eight percent of the gap nearest the pad for the width of the pad is supplied by cool oil at approximately supply oil temperature. Fluid mixing distribution at the pocket/pad feed plane shows a central region that has a mixture of 75 percent of the cool supply oil (Figure 24). Zones to each side of this have been completely mixed, 50 percent of the cool supply oil and 50 percent of the boundary oil. Zones at the extreme ends of the pad show 90 percent supply oil and 10 percent boundary oil due to geometry and speed effects.
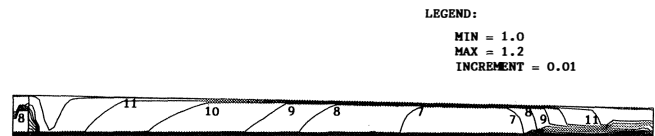
LEGEND:
MIN = 1.0
MAX = 1.2
INCREMENT = 0.01

Figure 23. Pad with Pocket Inlet Temperature for Laminar Flow.

LEGEND:
MIN = 0.02
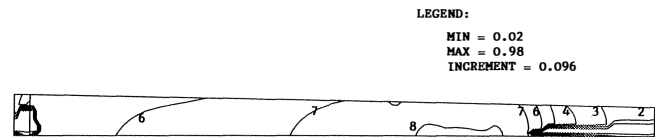MAX = 0.98
INCREMENT = 0.096

Figure 24. Pad with Pocket Inlet Mixing Field for Laminar Flow.

The CFD model for the turbulent Case B showed three vortices near outlet two with tighter radii compressed into a shorter radial distance than Case A (Figure 25). Velocity vectors are aligned radially to the outside of inlet two. Swirl is occurring at inlet two and two vortices are present towards the pad inside diameter that were absent in Case A. On the radial midplane, at inlet two, velocities are directed towards the runner for the full cavity depth (Figure 26). This is diverted to radial tangential flow near the runner to a greater extent to the outside of inlet two. Low velocity occurs at the cavity bottom. The outer vortex near the pad outside diameter is compressed and the adjacent vortex has started to dissipate. The transverse velocity field at the optimized pocket section was similar to Case A (Figure 27).

The turbulent Case B showed the larger temperature range (Figure 28). Outlet two flow was greater than Case A, because of the higher speed, and the cool oil region of the cavity was 25 percent greater than Case A in the axial planes (Figure 29). The main body of fluid in the optimized section transverse plan was also at approximately the same temperature as Case A (Figure 30).

The mixing plots show Case B inlet two fluid extending to the runner boundary fluid at inlet two. In Case A, the fluid entering at the feed is 70 percent of inlet two fluid directly above inlet two in the radial plane plots. Both axial and transverse planes show the 70 percent fluid inlet two Case A being double the volume in Case B (Figure 31 and 32). Fluid at the cavity inside diameter and outside diameter are at five percent to ten percent more fluid from inlet two. The transverse plots at the inner, mean, outer radius show less mixing for Case B. The outer plane is 83 percent, fluid inlet two at the bulk core for the high speed case *vs* 70 percent fluid inlet two of Case A (Figure 33).
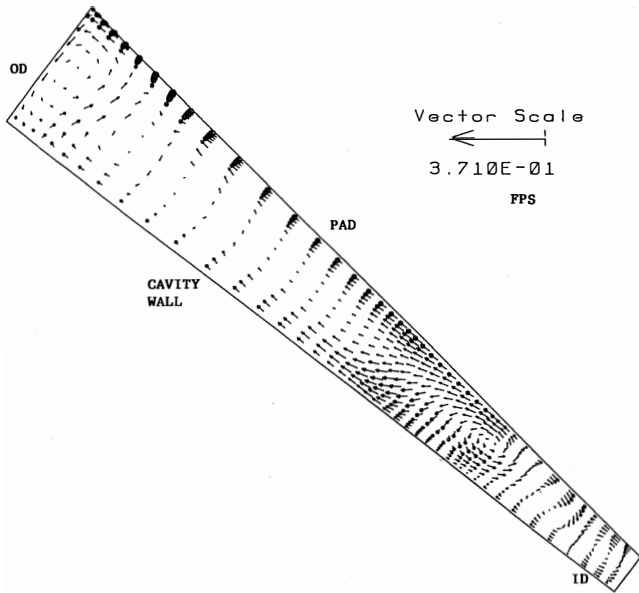
Figure 25. Controlled Inlet Pad Cavity Axial Mid Plane Turbulent Velocity Field (.188 in from Runner).
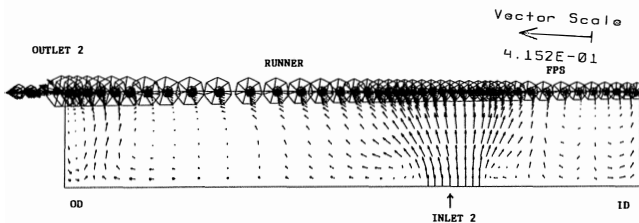

Figure 26. Controlled Inlet Pad Cavity Radial Mid Plane Turbulent Velocity Field.
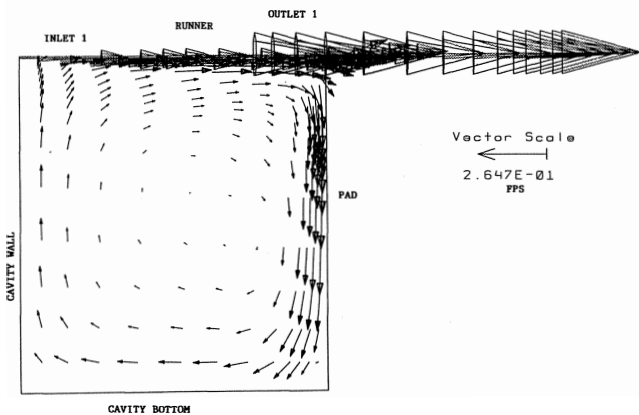

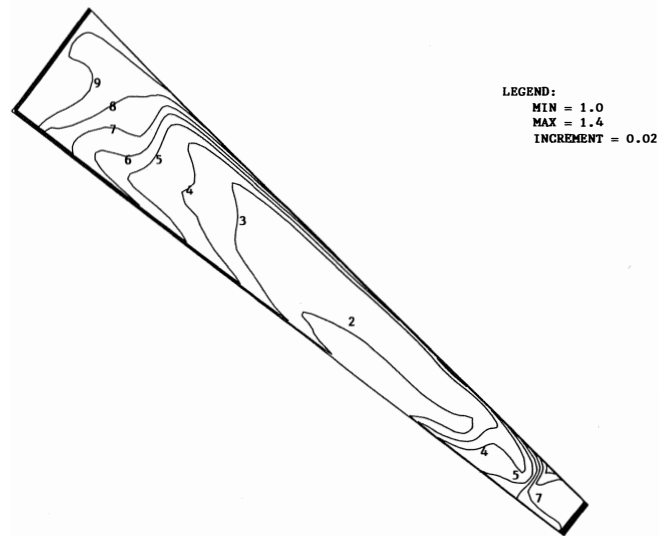*Figure 27. Controlled Inlet Pad Cavity Transverse Plane Turbulent Velocity Field (Radius = 4.54 in).*

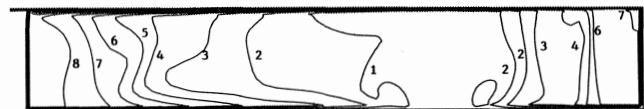*Figure 28. Controlled Inlet Pad Cavity Axial Mid Plane Temperature Distribution for Turbulent Flow.*

Figure 29. Controlled Inlet Pad Cavity Radial Mid Plane Temperature Distribution for Turbulent Flow.
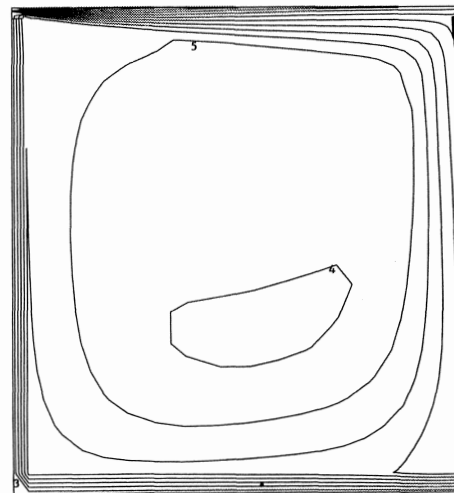

Figure 30. Controlled Inlet Pad Cavity Transverse Plane Temperature Distribution for Turbulent Flow.

Viscous heating for the turbulent model is occurring at the runner boundary and pad wall (Figure 34). The zone is approximately double the laminar model. At the inlet pad corner a larger zone of energy dissipation is occurring. The horsepower generated by the pocket is 0.043 per pad, which raises the oil temperature less than one-tenth of 1°F.

The pocket/pad feed interface plane outlet one, dominant velocity is about 30 percent of the runner mean velocity (Figure 35). The hot boundary layer is approximately nine percent of gap.

Backflow is occurring at the cavity outside diameter for two percent of the pad radial length and the full gap height below the runner boundary layer. Backflow is not occurring at the pad gap inside diameter as in the laminar case.

The pad inlet gap temperature distribution range is to 1.4 times the inlet temperature (Figure 36). The lower temperatures are near the pad and the highest temperatures are at the gap outside diameter and inside diameter near the runner. At inlet two in the gap and within 30 percent of the pad, the temperature is 1.10 times the inlet temperature for one-fourth of the pad radial length. The center one-third of the gap height at 1.16 times and the gap near the runner is at 1.4 times the feed temperature.
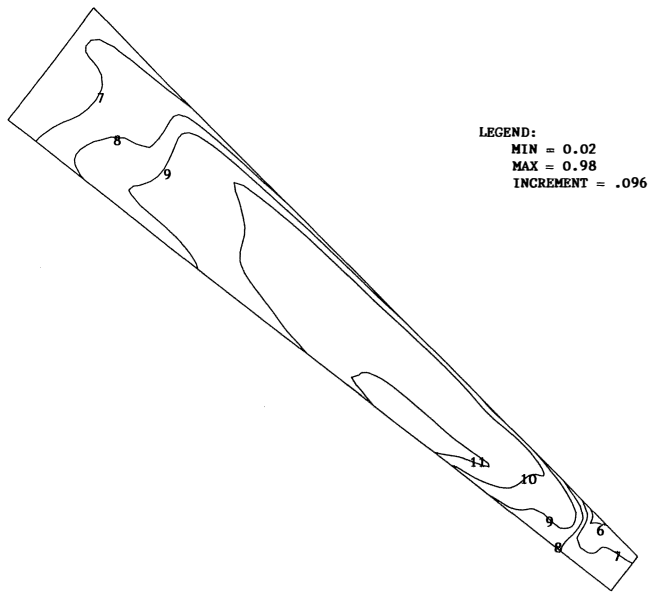
LEGEND:
MIN = 0.02
MAX = 0.98
INCREMENT = .096

Figure 31. Controlled Inlet Pad Cavity Axial Mid Plane Mixing Field for Turbulent Flow.
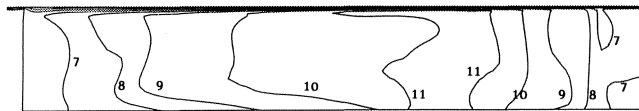

Figure 32. Controlled Inlet Pad Cavity Radial Mid Plane Mixing Field for Turbulent Flow.
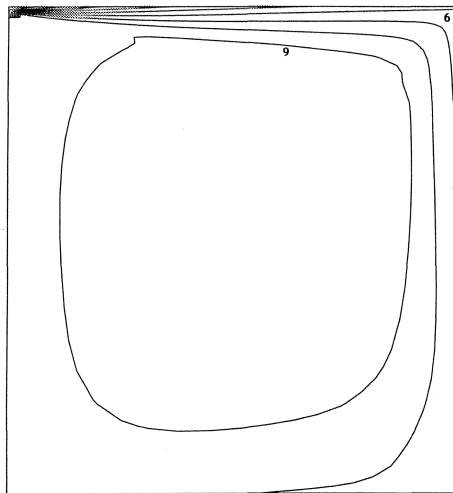

Figure 33. Controlled Inlet Pad Cavity Transverse Plane Mixing Field for Turbulent Flow.

Figure 34. Controlled Inlet Pad Cavity Transverse Plane Viscous Heating for Turbulent Flow.

LEGEND:
MIN = −0.40
MAX = +1.31
INCREMENT = 0.34
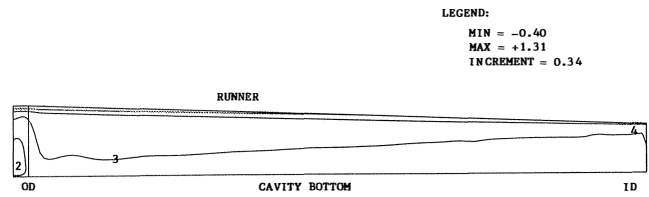
Figure 35. Pad with Pocket Inlet Velocity Field for Turbulent Flow (Pad Entrance Gap, Outlet 1).

LEGEND:
MIN = 1.0
MAX = 1.4
INCREMENT = 0.02
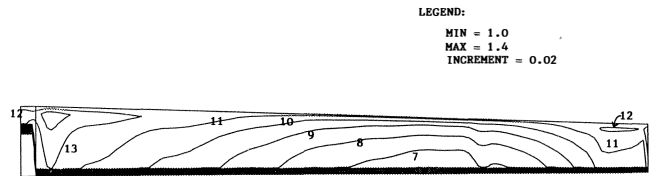
Figure 36. Pad with Pocket Inlet Temperature for Turbulent Flow.

LEGEND:
MIN = 0.02
MAX = 0.98
INCREMENT = 0.096
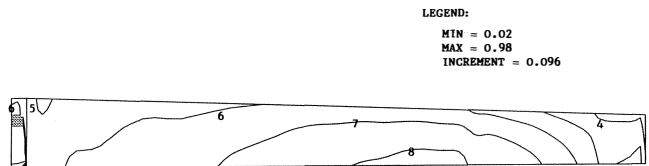
Figure 37. Pad with Pocket Inlet Mixing Field for Turbulent Flow.

The fluid mixing maps show a similar distribution as temperature maps at the pad feed plane (Figure 37). Fluid is 75 percent cavity feed fluid near the pad at cavity inlet two. The mixing near the runner is 50 percent of inlet two fluid. Towards the pad extremes the fluid is 30 percent of cavity feed fluid. The increased speed of runner B has resulted in less mixing, especially at the central pad area in the gap. Case B shows stratified temperature and mixing plots.

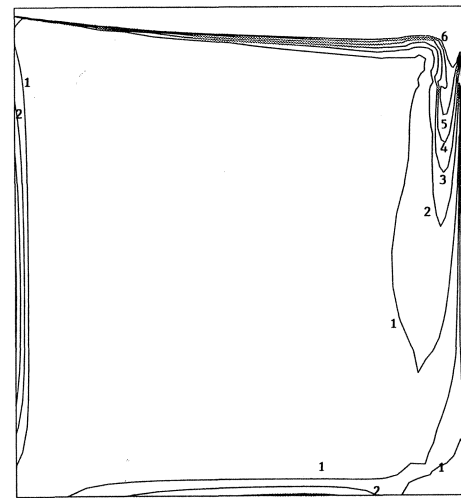For the laminar flow model, the average hot oil carryover temperature was reduced by 53 percent when mixed with the controlled inlet oil being fed at 120°F. For the turbulent model running 1.7 times faster, the hot oil carryover temperature was reduced by 56 percent.

Some of the data for the laminar and turbulent models are summarized in Table 5. The turbulent viscosity to oil viscosity ratio at the pad entrance and over the cavity domain are shown. Cavity swirl velocities are mass averaged values on a horizontal mid plane 0.1 in wide at the transverse plane at a radius of 4.54 in. Centrifugal fluid velocities are also shown.

Table 5. CFD Controlled Inlet Fluid Parameters.

CASE	FLOW	CAVITY SWIRL[Δ] VELOCITY		CAVITY CENTRIFUGAL VELOCITY		PAD ENTRANCE[*] TURBULENCE RATIO	CAVITY TURBULENCE RATIO
		IPS	% RUNNER SPEED	IPS	% RUNNER SPEED	DIM.	DIM.
A	LAMINAR	172	4.2	84	2.0	0.6	1.0
B	TURBULENT	235	5.7	152	3.7	1.5	2.0

*   MASS WEIGHTED AVERAGE

Δ   R = 4.54"

DESIGN FEATURES AND PERFORMANCE OF A CONTROLLED INLET BEARING

Controlled Inlet, Offset Pivot, and Copper Pads

Thrust bearings can feature offset pivot, chromium copper pads, or pad cool oil pockets individually or in combinations. Pad pivot offsets traditionally were under 60 percent, because various isoviscous analysis showed that optimum loading of tilt pads was occurring near an inlet to outlet film ratio of two. Since bearing failure is based on local babbitt temperature and film temperatures drop at higher pad inclinations, i.e., pivot offsets, by changing the criteria, greater pad offsets have become popular. A plot is shown in Figure 38 of local babbitt temperature *vs* pivot position at 500 psi loading and 6000 rpm. For the steel pads, babbitt temperature decreases to pivot offsets as high as 80 percent. Many bearings today have offsets between 65 percent and 70 percent.
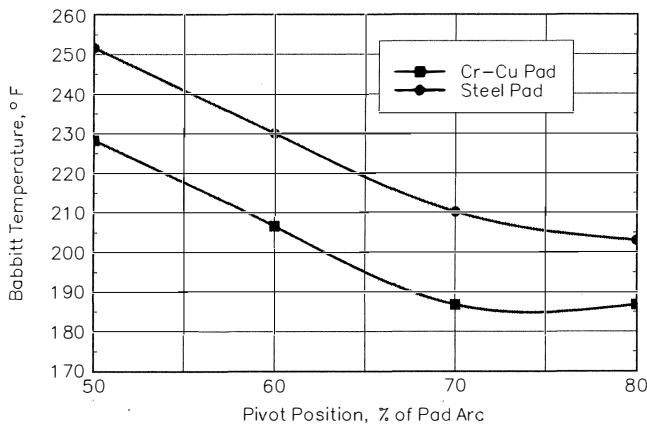

Figure 38. Pad Temperature Vs Pad Pivot Offset.

As pivot offset increases, the inclination of the pad to the rotating collar increases. This allows a higher volume of bearing feed oil to enter the pad compared to the carryover boundary layer oil. The shear rate of the lubricant is reduced, thus dropping the film temperature. The tradeoff is with babbitt creep at local sites on the pad. Design charts showing the babbitt yield strength *vs* temperature with a design safety factor allow the local babbitt pressure and temperature to be reviewed for different placements of the pivot. If the babbitt stress is approaching the yield limit of babbitt or creep initiation the percent of pivot offset can be reduced.

The material type also can reduce local babbitt temperatures. A drop in temperature of about 25°F is shown in Figure 38 by using a strengthened copper with one percent chromium in place of a steel for the pad backing material. The temperature reduction is due to the two effects. The higher thermal conductivity of copper, 190 BTU/hr-ft-°F as compared to steel 31 BTU/hr-ft-°F, reduces the temperature differential from the top to the bottom of the pad. This reduces the thermal crowning of the pad, which reduces the local babbitt temperature and pressure along with increasing the film thickness. A one dimensional thermal model also shows local babbitt temperatures being reduced directly. The temperature reduction changes with speed and load. It can be as great as 54°F at a load of 700 psi to no decrease at a load of 100 psi. Speed effects the temperature reduction, 36°F below 10,000 rpm and 18°F above. Copper does have an elastic modulus of 16.1 E6 psi, about one-half the modulus for steel. This allows for more crowning of the pad due to pad elasticity. When copper pads are at high loads, the pad crowning should be studied for loss of load capacity and film thickness. Pads can be redesigned with greater depth or a different support system to compensate for the loss of modulus.

The cool oil pocket features prepad mixing of boundary layer and bearing inlet oil. A standard bearing will mix the boundary layer with lubricant that is at a bulk oil temperature above the bearing inlet oil. The bulk temperature used is usually the bearing outlet temperature assuming a flooded bearing. This higher bulk temperature occurs because of the parasitic losses both through flow and surface area drag and mixing of the oil leaving the sides of the pad. Many bearings have a bulk temperature rise of 30°F with a bearing inlet temperature of 120°F. Thus, the standard flooded bearing mixes the hot boundary layer oil from the previous pad with 150°F oil; whereas the pocket or controlled inlet bearing mixes bearing inlet oil at 120°F with the boundary layer to determine pad inlet temperatures. Two other features of the controlled inlet bearing help reduce the pad inlet temperature: the hot oil director and wiper. The director moves previous pad side leakage oil to the collar area to be spun out of the bearing instead of raising the pad inlet oil temperature. The wiper, or controlled inlet land, will shed a portion of the boundary layer into the director stream. Since the wiper's distance to the collar is below but near the pad inlet film thickness, one to two ten thousands of an inch, a major portion of the boundary layer still enters the cool oil pocket to be mixed.

The offset pivot, copper material, and pad controlled inlet all appear to reduce pad babbitt temperature which is the prime indicator of bearing capacity. Using two or all three of the features does not mean that the temperature reduction of the film can be estimated by adding the features directly; since, they are related nonlinearly with interaction effects.

A Controlled Inlet Thrust Bearing

The controlled inlet bearing (Figure 39) has design features that increase load capacity along with reduce flow requirements and power consumption. The load capacity is augmented by three features: the controlled inlet (Figure 40) which consists of a hot oil director, wiper, and cool oil pocket; the offset pivot which tips the shoe to a greater inclination allowing more cool oil from the pocket to mix with the boundary layer hot oil; and the pad line contact support reduces radial pad deflection that button type supports inherently have. The reduced deflection translates into greater load capacity. The capacity can be as high as 750 psi unit load.

The flow requirements are reduced by the controlled inlet cool oil pocket that places and holds the cool oil at the pad front edge and the controlled inlet lubricant feed system that delivers the cool oil to the pocket. The oil containment by the controlled inlet and feed system reduce parasitic loss. Horsepower loss reduction is surface drag and through flow losses. Less oil is heated by shear at
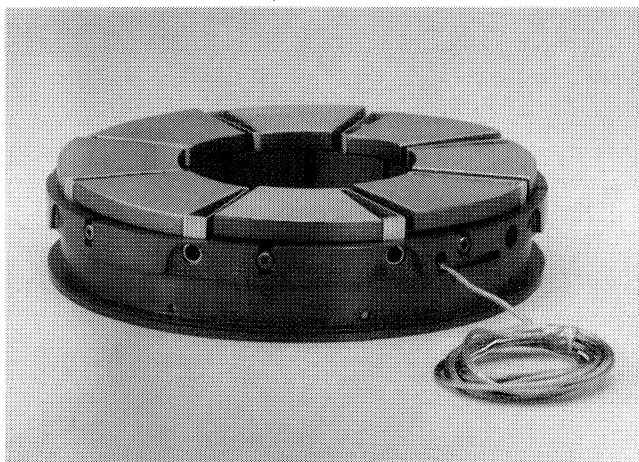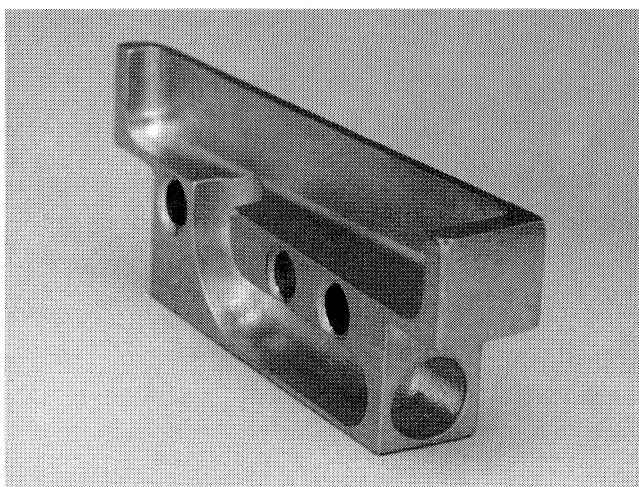
Figure 39. Controlled Inlet Thrust Bearing.

Figure 40. Controlled Inlet Showing Hot Oil Director Wiper and Cool Oil Pocket.

the shaft/retainer annulus and the collar housing annulus because of lower fluid velocities. Shoe side shear is still occurring at the front and rear of shoe. The entrance, between pad, and discharge entrance loses are less due to lower flows and fluid velocities.

Thin Axial Profile Bearing

The bearing assemble has a thin axial profile because the retainer (Figure 41) has an optional bottomless feature. Axial height is reduced 31 percent for the feature. This can reduce rotor length on new machines and will allow the bearing to be fit into all upgrade or rerate designs. The bottomless retainer produces a tighter stack height tolerance which allows the links to give a greater proportion of their adjustment range to misalignment duties as compared to manufacturing tolerance issues. By omitting the retainer trepan bottom with parallel, flatness, and tolerance issues which are occurring on the largest assembly part, and transferring tolerances to small parts, the stack height tolerance is reduced. The retainer bottom tolerance has been replaced by a dowel pin tolerance. Thus, the thin thrust bearing assemble is more accurately made and functions better for misalignment.

The retainer is not part of the axial load system with this bearing, it functions to hold bearing parts in the assembly. The retainer is replaced by the lower link dowel pin in the axial load system. The pin functions include transferring the axial load, positioning the
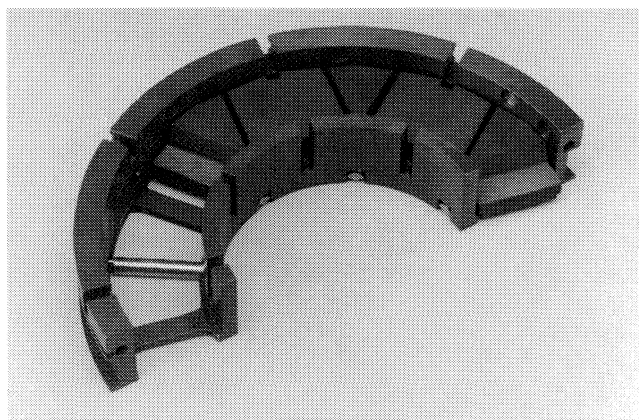

Figure 41. Controlled Inlet Thrust Retainer Showing Assembly of Lower Link Pin and Links.

retainer in the housing, locating the lower link circumferentially, securing it against rotation, and holding the assembly together for shipping and turbomachine assembly.

Pad

The radial rib with line contact has replaced the spherical pivot with point contact which reduces radial elastic pad deflection, thus increasing load capacity or film thickness and results in lower babbitt temperatures. The pad and other components are retained by a screw lock that prevents parts falling out at assembly.

Controlled Inlet

The controlled inlet feeds each pad front edge (Figure 42). The fluid flows radially in and axially up to the cool oil pocket. In the pocket, the cool oil mixes circumferentially by swirl and radially by centrifugal forces with the boundary layer hot oil carryover. The pocket cross section has optimized mixing geometry at the outer one-third of the pad front edge since this section requires the most flow and develops the highest local temperatures downstream, near the trailing edge of the pad.
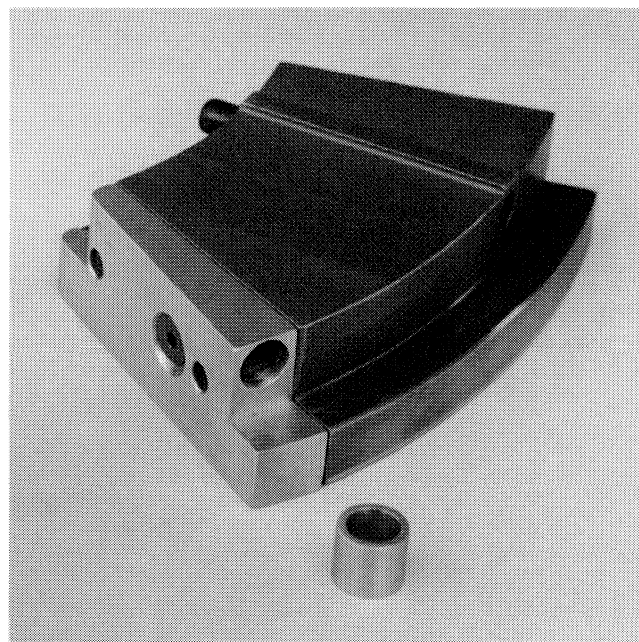

Figure 42. Pad with Controlled Inlet and Lube Feed Piston.

The controlled inlet consists of a precavity and hot oil director that move some of the hot oil from the previous pad radially out of the bearing in the precavity. The land or wiper also reduces the carryover oil to the pocket by shedding some of the boundary fluid at the wiper front edge to the precavity. The reduced boundary layer is then mixed in the pocket cavity with cool inlet oil to enter the pad.

The controlled inlet is made of babbitt so that the runner "sees" only soft babbitt as the pad surface. The controlled inlet is detachable so that a flooded or controlled inlet bearing differ only by adding the controlled inlet and pistons. This allows for easy upgrades in the field, if desired.

Piston

The controlled inlet pocket feed system includes the retainer circumferential annulus and an axial half cylinder with large corner radii for reduced pressure losses to feed the radial floating bronze hollow piston. The piston is located in the retainer and moves radially by differential hydraulic forces to seal against the controlled inlet. This design is easier to assemble and has fewer parts or higher assembly reliability. The large bore diameter of the piston, half cylinder ports in the retainer, and large turning radius in the controlled inlet have reduce feed system pressure drop.

Links

The links (Figure 43) are designed to provide a misalignment capacity. Contact stresses are lower where a pair member is made of a soft material, at the pad/upper link interface and the lower link/link pin/housing interface. Higher contact stresses exist by design where the pair members are both hard, that is upper link/lower link contact. At current thrust bearing catalog loads, 500 psi, the pad/upper link contact stress is 50 percent of the spherical pivot contact stress. The lower link support pin and support pin/housing or shim contact stress is 70 percent and 10 percent of the lower link/retainer, cylinder on plate contact stress.
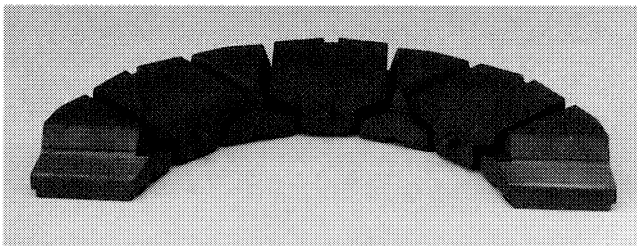

Figure 43. Controlled Inlet Thrust Bearing Upper and Lower Link Assembly.

Performance of a Controlled Inlet Bearing

A controlled inlet bearing with offset pivot will have higher capacity, lower power losses, or a combination of both. The following discussion tries to show the interplay of load, speed, and flow in the bearing performance parameters, horsepower loss, and babbitt local temperature. Figures 44 through 47 should be viewed simultaneously. That is, for a given speed, load, and flow (Figure 44 and Figure 45), the resulting babbitt temperature and horsepower loss (Figures 46 and 47) may be determined. Most published thrust bearing data does not show flow effecting local temperature. The load/speed map is shown in Figure 44 for a 10-1/2 in thrust bearing running at base conditions, 30 percent more load, and 50 percent less flow. The speed range is 2000 to 8000 rpm and loading is to 39000 pounds at the higher speed. The required flow is shown in Figure 45 for the three cases: base condition, high load, low flow.
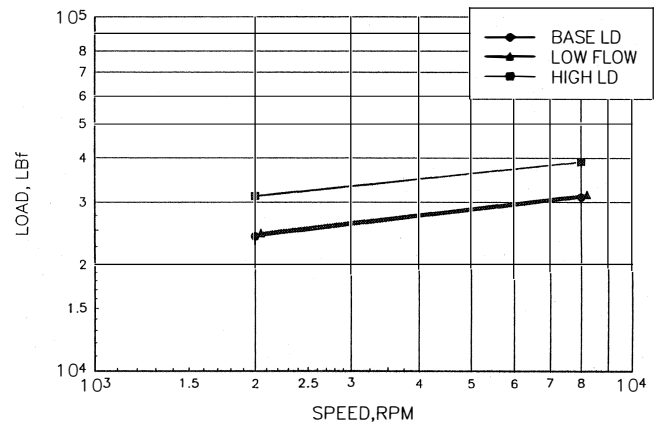

Figure 44. Load Vs Speed, 10-1/2 in Thrust Bearing with Pocket Inlet, Offset Pivot, and Steel Pads.
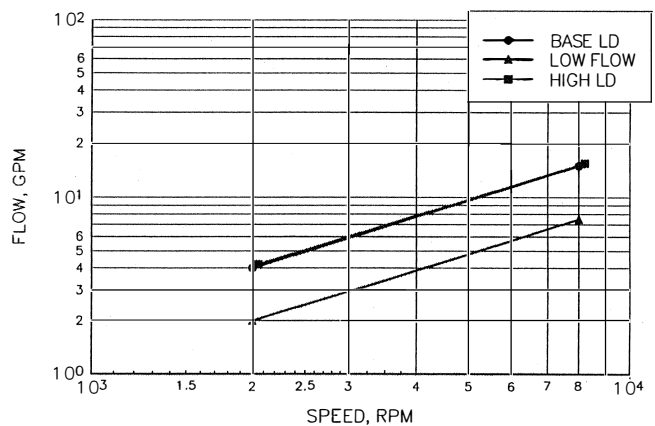

Figure 45. Flow Vs Speed, 10-1/2 in Thrust Bearing with Pocket, Offset Pivot, and Steel Pads.
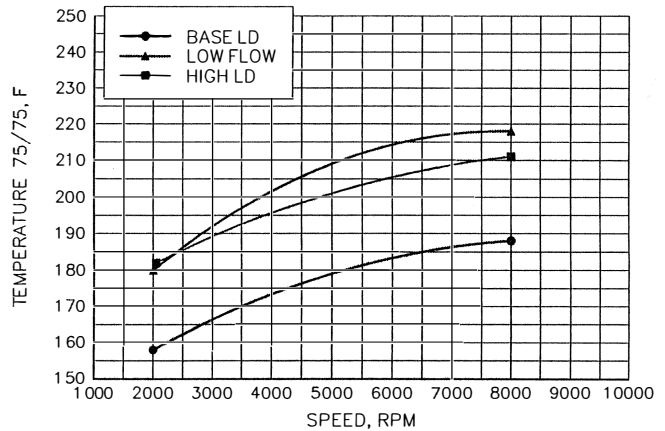

Figure 46. Pad Temperature, 10-1/2 in Thrust Bearing with Pocket, Offset Pivot, and Steel Pads.

The babbitt temperature plot (Figure 46), which is a good indication of bearing capacity, shows an average temperature difference at 2000 rpm of 22°F when comparing either the high load or low flow bearing to base conditions. At a higher speed of
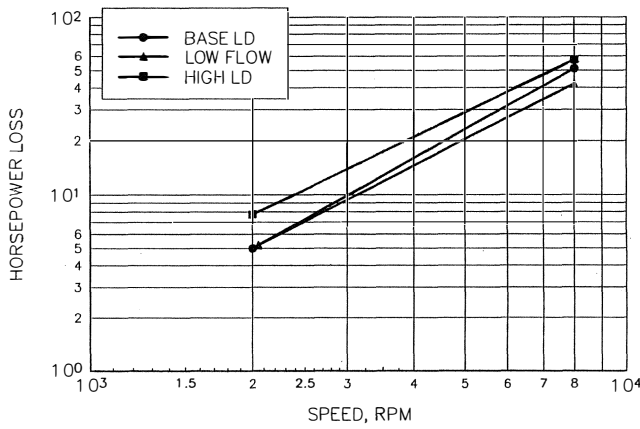
Figure 47. Horsepower Loss Vs Speed, 10-1/2 in Thrust Bearing with Pocket, Offset Pivot, and Steel Pads.

8000 rpm, the average difference between the high load or low flow and the base bearing is 27°F. In a more general plot (Figure 49), the local temperature increases with reduction in bearing flow requirement. A standard lug type bearing with center pivot running flooded has a higher local pad temperature and cannot be operated to as low a flow as a controlled inlet bearing. The latter bearing with both the advantage of pad pivot offset that allows more cool oil to enter the front of the pad, because that edge has dropped farther from the runner, and the control of cool inlet oil at the front of the pad by the pocket allow for lower measured temperature.

Parasitic horsepower loss is correlated with speed and flow. By reducing the flow, the bearing horsepower loss is less. Assuming a bulk temperature rise of 40°F to 50°F, which is common for controlled inlet bearings, reductions in flow can reduce bearing horsepower loss, provided of course, flow reductions do not go below the minimum flow requirement for hydrodynamic lubrication. The horsepower loss, shown in Figure 47, for base and low flow bearings being approximately the same at 2000 rpm, since at low speeds parasitic losses are not significant when compared to the hydrodynamic pad shearing loss. At 8000 rpm, the horsepower was reduced by 18 percent for the low flow bearing. Larger reduction will occur at higher speeds. Horsepower loss vs bearing supply flow is shown in Figure 48. Here, horsepower loss drops by 40 percent as the flow is reduced from 40 gpm to 7-1/2 gpm, at a 300 psi load, and a speed of 8000 rpm.
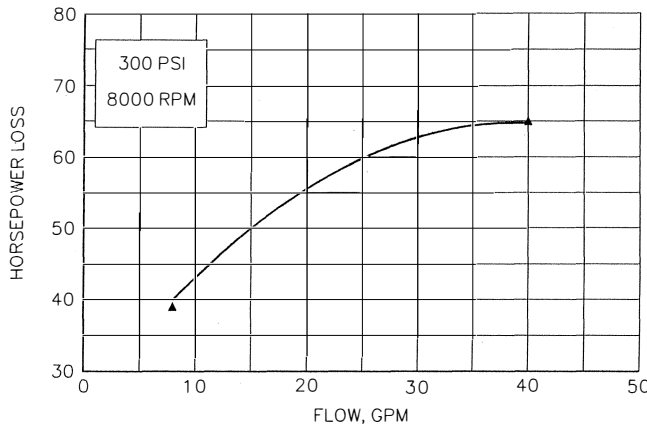

Figure 48. Horsepower Loss Vs Flow, 10-1/2 in Thrust Bearing with Pocket, Offset Pivot, and Steel Pads.
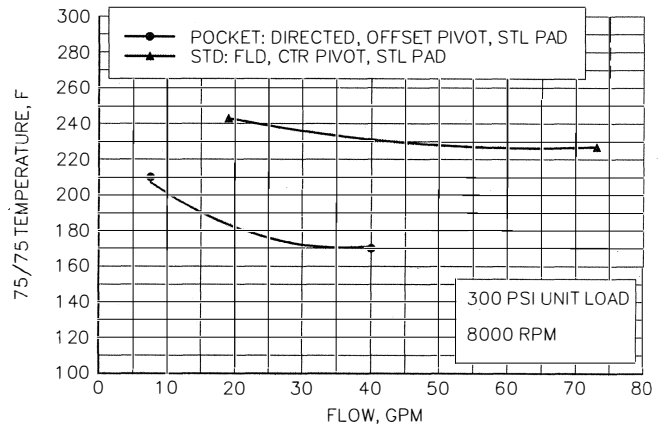

Figure 49. Pad Temperature Vs Flow, 10-1/2 in Thrust Bearing, Flooded Vs Pocket.

CONCLUSIONS
Tilt Pad Thrust Bearing Selection

• With Just in Time manufacturing, manufacturing cells, short lead time NC machined bearing components, and engineering tools like CFD, thrust bearings can be designed for the application rather than having to use a catalog item.

• Establish what parameters control bearing capacity by plotting bearing on the load speed map and using Table 1.

• Ask bearing supplier what type of analysis was used. As the solution includes more variables, it emulates run conditions closer.

   • Isoviscous approximation by closed form solutions for film, i.e., short or long bearing theory

   • Isoviscous hydrodynamic film solution

   • Thermohydrodynamic film solution

   • Thermohydrodynamic film solution with turbulence

   • Thermohydrodynamic film solution with turbulence and pad thermal effects

   • Thermohydrodynamic film solution with turbulence and pad elastic effects

   • Thermohydrodynamic film solution with turbulence and pad thermal and elastic effects

   • Thermohydrodynamic film solution with turbulence and pad and runner thermal and elastic effects

   • CFD coupled thermohydrodynamic film solutions with turbulence and pad and runner thermal and elastic effects

• Review design features with bearing suppliers to determine bearing capacity, features as pad ratio and pad spacing. Discuss pivot position strategy, pad crowning criteria, etc. Establish the special features you need for your bearing application, such as no load axial vibration control or a particular film thickness ratio for a process fluids application.

Pad Entrance Temperatures

• The two dimensional array, temperature field, at the pad entrance is determined by a CFD analysis of the controlled inlet pocket flows. Previous procedures to determine pad entrance temperature have produced an average value of temperature. Bearing capacity is partially determined by an accurate pad inlet temperature.

• Using an inlet temperature distribution rather than an average inlet temperature should predict babbitt temperatures more

accurately. With the ability to view the pad entrance gap as a two dimensional field of temperatures, it appears that the boundary layer near the runner can be above the babbitt limit temperature because the fluid near the pad babbitt is at a lower temperature for highly loaded bearings.

• CFD analysis can be used to design an optimum cavity for a specific load/speed envelope.

• The cavity transverse swirl is optimum at the pad entrance radius where the highest pad pressure occurs downstream. A swirl rotational velocity reduces pad inlet temperatures by interacting and shedding a portion the boundary layer. A higher degree of mixing occurs at the optimized plane compared to the mean and inner transverse plane.

• The controlled inlet cavity cool oil entrance is optimally placed so the lowest pad inlet temperature field is where the pad will see the highest local temperatures and pressures downstream.

• The cavity velocity maps were similar qualitatively for the laminar and turbulent cases.

• The turbulent case with increased feed due to the speed had filled more of the cavity volume with cool oil.

• Higher inlet flows will cause less mixing resulting in a temperature stratification at the pad entrance. This is occurring in the circumferencial and axial plane of the cavity.

• CFD bearing analysis can be used to estimate internal bearing parasitic power losses.

Controlled Inlet Thrust Bearing Features

• Higher capacity by design, 50 percent more. Higher bearing capacity due to offset pivot pad and controlled inlet design, 750 psi.

• Low stack height due to retainer construction, 31 percent less.

• Lower feed flow requirement due to controlled inlet, 40 percent less.

• Lower horsepower loss due to reduced flows and lower surface drag and through flow power loss, 20 percent less.

• Lower Hertz contact stress in links due to conformable surfaces or line contacts replacing spherical pivot contacts in soft pairs.

• Modularity of controlled inlet allows for field retrofits for increased load or reduced horsepower losses.

• The hydraulic feed piston and controlled inlet oil pocket supply cool oil to the front pad edge with fewer parts and a simpler assembly.

• The controlled inlet functions as a collar wiper, director for hot oil carryover, and cool oil supply cavity for the pad.

NOMENCLATURE

B_i = Body force
C_1 = Constant
C_2 = Constant
C_u = Constant
C_p = Specific heat
E_G = Groove energy sink
E_P = Pad energy sink
E_R = Runner energy sink
E_S = Side leakage energy sink
E_T = Shear energy source
g_i = Gravitational force
H = Total enthalpy
h = Enthalpy
K = Conductivity

$$K_1 = \frac{T_1 - T_s}{T_r - T_s}$$

k = Turbulent kinetic energy
m_i = Mass at inlet i
Pr_t = Turbulent Prandtl number
p = Pressure
Q_1 = Flow to pad
Q_2 = Flow from pad
Q_r = Recirculation flow
Q_s = Bearing supply flow
S = Source terms
T = Temperature
T_1 = Fluid temperature at pad entrance, °F
T_2 = Fluid temperature at pad exit, °F
T_r = Runner temperature, °F
T_s = Fluid supply temperature, °F

$\left.\begin{matrix} u_i \\ u_j \\ u_k \end{matrix}\right\}$ = 3 dimensional orthogonal velocities of a spacial position in the fluid

u_i' = Fluctuating velocity component
$\bar{u}_i$ = Mean fluctuating velocity component

$\left.\begin{matrix} x_i \\ x_j \\ x_k \end{matrix}\right\}$ = 3 dimensional orthogonal velocities of a spacial position in the fluid

Γ = Diffusion coefficient, K/cp
ΔT = Temperature rise along pad streamline, °F
ε = Turbulent kinetic energy dissipation rate
λ = Mixing constant
μ = Viscosity
μ_e = Effective viscosity
μ_t = Turbulent viscosity
ρ = Fluid density
σ_k = K-ε Schmidt number
σ_ε = K-ε Schmidt number
τ = Fluid stress
ϕ = Mass fraction

APPENDIX

Computational fluid dynamics equations for laminar and turbulent steady state flow are shown below. The terms in the equations are in the NOMENCLATURE section.

Reynolds Equation

$$\frac{\partial}{\partial x}\left(\frac{G_{\chi_i} h^3}{\mu} \frac{\partial P}{\partial \chi_i}\right) + \frac{\partial}{\partial \chi_j}\left(\frac{G_{\chi_j} h^3}{\mu} \frac{\partial P}{\partial \chi_j}\right) = \frac{U}{2}\frac{\partial h}{\partial \chi} \qquad \text{A-1}$$

For Laminar Flow
Conservation of Mass

$$\frac{\partial(\rho u_i)}{\partial x_i} + \frac{\partial(\rho u_j)}{\partial x_j} + \frac{\partial(\rho u_k)}{\partial x_k} = 0 \qquad \text{A-2}$$

Conservation of Momentum

$$\frac{\partial(\rho u_i)}{\partial t} + \frac{\partial(\rho u_i u_j)}{\partial x_j} = B_i + \frac{\partial \tau_{ij}}{\partial x_j} \qquad \text{A-3}$$